PHYSICAL REVIEW C **80**, 021303(R) (2009)

Triaxial rotor model description of quadrupole interference in collective nuclei: The P_3 term

J. M. Allmond,[1,2] J. L. Wood,[2] and W. D. Kulp[2]
[1]*Department of Physics, University of Richmond, Virginia 23173, USA*
[2]*School of Physics, Georgia Institute of Technology, Atlanta, Georgia 30332, USA*
(Received 9 June 2009; published 18 August 2009)

The triaxial rotor model with independent inertia and electric quadrupole tensors is applied to the P_3 term, $P_3 = \langle 0_1||\hat{T}(E2)||2_1\rangle\langle 2_1||\hat{T}(E2)||2_2\rangle\langle 2_2||\hat{T}(E2)||0_1\rangle$, which is a standard measure of quadrupole interference in collective nuclei. It is shown that the model naturally explains nuclei with anomalous signs for their P_3 terms. Measurements of $Q(2_1)$ in multiple-step Coulomb excitation can be significantly dependent on the sign of this term. The example of ^{194}Pt is considered.

DOI: 10.1103/PhysRevC.80.021303 PACS number(s): 21.60.Ev

Recently we have introduced a triaxial rotor model with independent inertia and electric quadrupole tensors [1]. This model has been applied to a detailed description of $E2$ matrix elements in the osmium isotopes [2]. An important ingredient of the model is the explicit description of interference effects that result between the inertia tensor and the electric quadrupole tensor. In the present study we apply the model to the P_3 term, which is a widely used [3–10] standard measure of quadrupole interference in collective nuclei, and we show that it provides a straightforward explanation of P_3-term sign anomalies without the need for higher order deformation terms such as β_4 used by Baker [11,12]. It is important to have reliable knowledge of the signs of P_3 terms because this can strongly influence the extraction of $Q(2_1^+)$ values from Coulomb excitation data [3,4,9,13–15].

The P_3 term,

$$P_3 = \langle 0_1||\hat{T}(E2)||2_1\rangle\langle 2_1||\hat{T}(E2)||2_2\rangle\langle 2_2||\hat{T}(E2)||0_1\rangle, \quad (1)$$

which is independent of the wave function phases but not the i^λ phase (i.e., $i^\lambda\langle I'||\hat{T}(E2)||I\rangle$, which is sometimes included in the definition of $E2$ matrix elements [16]), is straightforwardly calculated in any model of a nucleus exhibiting quadrupole collectivity. Early models that addressed this included the anharmonic vibrator model [17], the triaxial rotor model (with irrotational flow moments of inertia) of Davydov and Filippov [18], and the pairing-plus-quadrupole model of Kumar and Baranger [3]: all give a negative value for the related quantity

$$P_4 = \langle 2_1||\hat{T}(E2)||2_1\rangle P_3, \quad (2)$$

which is independent of all phase-factor conventions for the $E2$ matrix elements. The importance of this issue for extracting $Q(2_1^+)$ values from Coulex data is that the direct path to the 2_1^+ state, wherefrom reorientation depends on $\langle 2_1||\hat{T}(E2)||2_1\rangle$, is interfered with by the 0_1-2_2-2_1 path resulting in up to 40% uncertainties [3,4,9,13–15]. Such uncertainties can yield ambiguities in sign changes of $Q(2_1^+)$ as a function of nucleon number, which impacts the location of prolate-oblate shape ("phase") changes in nuclei (see, e.g., Ref. [19]).

The model [1] expressions for the matrix elements relevant to the present investigation are

$$\langle 0_1||\hat{T}(E2)||2_1\rangle = \sqrt{\frac{5}{16\pi}}\,Q_0\cos(\gamma+\Gamma), \quad (3)$$

$$\langle 0_1||\hat{T}(E2)||2_2\rangle = \sqrt{\frac{5}{16\pi}}\,Q_0\sin(\gamma+\Gamma), \quad (4)$$

$$\langle 2_1||\hat{T}(E2)||2_2\rangle = \sqrt{\frac{25}{56\pi}}\,Q_0\sin(\gamma-2\Gamma), \quad (5)$$

and

$$\langle 2_1||\hat{T}(E2)||2_1\rangle = -\sqrt{\frac{25}{56\pi}}\,Q_0\cos(\gamma-2\Gamma) = -\langle 2_2||\hat{T}(E2)||2_2\rangle, \quad (6)$$

where $Q_0 \propto \beta_2$ is the intrinsic quadrupole deformation measured in e b, the angle γ describes the triaxiality of the electric quadrupole tensor, and Γ is a mixing angle that depends on the triaxiality of the inertia tensor. Equations (3)–(6) are usefully depicted as shown in Fig. 1. The corresponding quadrupole moments are

$$Q(2_1^+) = \sqrt{\frac{16\pi}{5}}\frac{1}{\sqrt{2I_i+1}}\langle 22;20|22\rangle\langle 2_1||\hat{T}(E2)||2_1\rangle = -\frac{2}{7}Q_0\cos(\gamma-2\Gamma) = -Q(2_2^+). \quad (7)$$

The $i^\lambda = -1$ phase [16] is not used for the matrix elements in the present model. The convention for prolate and oblate shapes follows that of Bohr and Mottelson [20] and of Davydov and Filippov [21] (i.e., $\gamma = 0°$–$30°$ for prolate shapes, $\gamma = 30°$–$60°$ for oblate shapes, and so forth by use of the $D2$ symmetry group). However, in practice, fitting oblate nuclei to Fig. 1 is done by using the $\gamma = 0°$–$30°$ range with a negative intrinsic deformation, $-|Q_0| \propto -|\beta_2|$, which preserves the three-axis as the basis, $|IK\rangle$. From that point, one can map to the $\gamma = 30°$–$60°$ range with $+|Q_0| \propto +|\beta_2|$

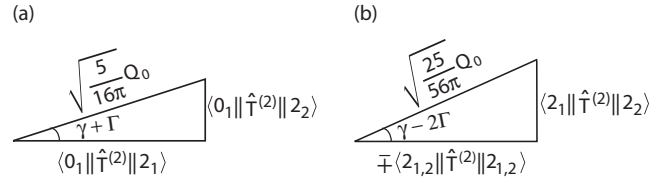

FIG. 1. The geometric representation of the model parameters and $I = 0, 2$ subspace.

by $60^\circ - \gamma$ and $-60^\circ - \Gamma$. The two choices for describing oblate nuclei are equivalent except for the ordering of the axes which is experimentally indistinguishable. Because the $E2$ properties of prolate and oblate nuclei are symmetric about $\gamma = 30^\circ$ (except for the sign of the quadrupole moments) [21], we confine the use of γ to the 0°–30° range and use $+|Q_0| \propto +|\beta_2|$ for prolate nuclei and $-|Q_0| \propto -|\beta_2|$ for oblate nuclei.

From Eqs. (3)–(6), one directly obtains

$$P_4 = \frac{125}{7168\pi^2} Q_0^4 [\cos(4\gamma - 2\Gamma) - \cos 6\Gamma], \tag{8}$$

which is zero when $\gamma = |\Gamma|$, negative when $\gamma > |\Gamma|$, and positive when $\gamma < |\Gamma|$ for the $0^\circ \leqslant \gamma \leqslant 30^\circ$ region. Because $P_4 \propto Q_0^4 \propto \beta_2^4$, the sign of P_4 is phase independent and, therefore, strictly determined by the relative amount of $E2$ and inertial asymmetry, γ and Γ, respectively. In fact, the sign of P_4 can be determined from Fig. 1(a) alone [i.e., it is the $\langle 0_1||\hat{T}(E2)||2_2\rangle \propto \sin(\gamma + \Gamma)$ matrix element that is responsible for the change in sign]. The P_4 term is depicted in Fig. 2 and the phase conventions for the present model are given in Table I. For irrotational flow,

$$\Gamma_{\text{irrot}} = -\frac{1}{2}\cos^{-1}\left(\frac{\cos 4\gamma + 2\cos 2\gamma}{\sqrt{9 - 8\sin^2 3\gamma}}\right), \tag{9}$$

one obtains that P_4 is always <0, as noted above.

The nuclei ^{192,194}Pt are examples where $P_4 > 0$ is observed [6,8,10]. To our knowledge these are the only examples for which an anomalous $P_4 > 0$ is certain. Other possibilities for $P_4 > 0$ include ^{196}Pt [22] and ^{66}Zn [23], but because $\langle 0_1||\hat{T}(E2)||2_2\rangle \sim 0$, the experimental errors make the sign ambiguous. There has also been a recent study of ^{74,76}Kr, where $P_4 > 0$ with respect to both 2_2 and 2_3. However, the K assignments appear ambiguous because of strong mixing of $K = 0$, 2 and of prolate/oblate shapes; shape mixing is outside of the present description and 2_2 states that are $K = 0$ provide $P_4 > 0$ naturally [3]. While this is the limit of our

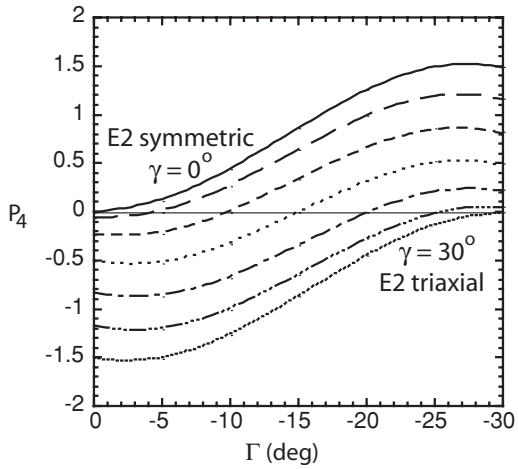

FIG. 2. The P_4 term, without the scale factor of $(125/7168\pi^2)Q_0^4$, is shown as a function of Γ for different values (0°, 5°, 10°, 15°, 20°, 25°, 30°) of triaxiality, γ. $P_4 = 0$ at $\gamma = |\Gamma|$. Both prolate and oblate nuclei are described in this $0^\circ \leqslant \gamma \leqslant 30^\circ$ region; see text for details.

TABLE I. The P_3 and P_4 sign convention for the region $0^\circ \leqslant \gamma \leqslant 30^\circ$, where oblate $E2$ shapes are generated in this region by use of a negative β (i.e., $-\beta_2 \propto -Q_0$, which preserves the three-axis as the basis, $|I\,K\rangle$).

P_3 (Triaxial sign convention—no $i^\lambda = -1$ phase)		
	$\gamma > \|\Gamma\|$	$\gamma < \|\Gamma\|$
$+Q_0$ (prolate)	+	−
$-Q_0$ (oblate)	−	+
P_4 (Triaxial sign convention—phase independent)		
	$\gamma > \|\Gamma\|$	$\gamma < \|\Gamma\|$
$+Q_0$ (prolate)	−	+
$-Q_0$ (oblate)	−	+

knowledge on known examples of $P_4 > 0$, future experiments should especially pay attention to the possibility of $P_4 > 0$ for the Hg isotopes, other Pt isotopes, and neutron-rich Os isotopes.

The present investigation focuses on explaining the $P_4 > 0$ anomaly for ^{194}Pt, where the 2_2 state is spectroscopically known to be $K = 2$. It has been studied by many groups using multi-Coulex [6,10,13,19,24–30]. Multi-Coulex studies provide the key quantity, $\langle 2_1||\hat{T}(E2)||2_1\rangle$, in P_4 and they contribute to the values of $\langle 0_1||\hat{T}(E2)||2_1\rangle$, $\langle 2_1||\hat{T}(E2)||2_2\rangle$, and $\langle 0_1||\hat{T}(E2)||2_2\rangle$. The value used here for $\langle 0_1||\hat{T}(E2)||2_1\rangle$ is computed from the evaluation of $B(E2; 0_1 \rightarrow 2_1)$ by Raman *et al.* [31], which gives $\langle 0_1||\hat{T}(E2)||2_1\rangle = 1.281^{9}_{8}$ e b. The measurements contributing to $\langle 2_1||\hat{T}(E2)||2_2\rangle$ and $\langle 0_1||\hat{T}(E2)||2_2\rangle$ are given in Table II and are from γ-ray yields following multi-Coulex [24–26,28], magnetic analysis of multi-Coulex scattered ions [27,29], and lifetime measurements using fast electronic timing [32]. The matrix elements $\langle 2_1||\hat{T}(E2)||2_1\rangle$ and $\langle 2_2||\hat{T}(E2)||2_2\rangle$ are also given in Table II and depend entirely on multi-Coulex measurements [13,24,25,29,30].

The model parameters Q_0, γ, and Γ can be determined for ^{194}Pt as follows. Using the triaxial parameter space outlined in Fig. 1 and the linearly weighted experimental $E2$ matrix elements in Table II, the model parameters Q_0 and $\gamma + \Gamma$ can be determined from Fig. 1(a) by

$$\begin{aligned} Q_0^{'} &= -\frac{1}{0.3154}\sqrt{(-1.281)^2 + (+0.091)^2} \\ &= -4.072^{28}\ \text{e b}, \end{aligned} \tag{10}$$

$$\begin{aligned} (\gamma + \Gamma)^{'} &= \arctan\left(\frac{+0.091}{-1.281}\right) \\ &= -4.06^{10}\ \text{deg}. \end{aligned} \tag{11}$$

The model parameters Q_0 and $\gamma - 2\Gamma$ can be determined from Fig. 1(b) by

$$\begin{aligned} Q_0^{''} &= -\frac{1}{0.3770}\sqrt{(-0.61)^2 + (-1.53)^2} \\ &= -4.37^{14}\ \text{e b}, \end{aligned} \tag{12}$$

TABLE II. Experimental $E2$ matrix elements, in e b, involving the 2_1 and 2_2 states in ^{194}Pt.

$\langle 0_1\|\|\hat{T}(E2)\|\|2_1\rangle$[a]	$\langle 0_1\|\|\hat{T}(E2)\|\|2_2\rangle$[a]	$\langle 2_1\|\|\hat{T}(E2)\|\|2_2\rangle$[a]	Source
1.281^{9}_{8}			[31]
	0.0888^{12}_{12}	1.517^{11}_{18}	[24]
	0.090^{2}_{2}	1.455^{25}_{25}	[25]
	0.098^{7}_{7}	1.72^{11}_{11}	[32,33]
	0.084^{6}_{6}	1.70^{10}_{10}	[26]
	0.097^{7}_{7}		[27]
	0.105^{9}_{9}		[28]
$(-)\,1.281^{9}$	$(+)\,0.091^{2}$	$(-)\,1.53^{5}$	Lin. Wt.
	$\langle 2_1\|\|\hat{T}(E2)\|\|2_1\rangle$	$\langle 2_2\|\|\hat{T}(E2)\|\|2_2\rangle$	Source
	$+0.63^{18}_{18}$		[29]
	$+0.59^{10}_{10}$		[30]
	$+0.54^{8}_{6}$	-0.40^{12}_{5}	[24]
	$+0.84^{21}_{21}$	-0.83^{8}_{8}	[13]
		-0.66^{60}_{60}	[25]
	$+0.61^{6}$	-0.66^{14}	Lin. Wt.

[a]The signs of individual off-diagonal or transitional $E2$ matrix elements are not observables (unlike the diagonal $E2$ matrix elements). However, the sign for the product of these matrix elements, P_3, is an observable. Because the signs are arbitrary to the degree that they give the correct P_3 sign, a negative sign $(-)$ is adopted here for $\langle 0_1||\hat{T}(E2)||2_1\rangle$ and $\langle 2_1||\hat{T}(E2)||2_2\rangle$ to comply with the convention $-\beta_2 \propto -Q_0$, $\gamma = 0^\circ$–30°, which forces $\langle 0_1||\hat{T}(E2)||2_2\rangle$ to be positive $(+)$.

$$(\gamma - 2\Gamma)'' = \arctan\left(\frac{-1.53}{-0.61}\right) = 68.1^{19}\ \text{deg}, \tag{13}$$

and

$$Q_0''' = -\frac{1}{0.3770}\sqrt{(-0.66)^2 + (-1.53)^2} = -4.41^{19}\ \text{e b}, \tag{14}$$

$$(\gamma - 2\Gamma)''' = \arctan\left(\frac{-1.53}{-0.66}\right) = 66.7^{46}\ \text{deg}. \tag{15}$$

This gives the final model values $Q_0 = -4.155^{98}$ e b, $\gamma = 19.85^{13}$ deg, and $\Gamma = -23.92^{13}$ deg (i.e., after taking linearly weighted averages of the redundantly obtained parameters) or, equivalently, $Q_0 = +4.155^{98}$ e b, $\gamma = 40.15^{13}$ deg, and $\Gamma = -36.08^{13}$ deg. Although only three matrix elements are needed to obtain the model parameters, the procedure used above provides an averaged fit to the $I = 0, 2$ subspace using all the data available. We note that the adopted *Nuclear Data Sheets'* [33] branching ratio, $I_\gamma(2_2 \to 0_1)/I_\gamma(2_2 \to 2_1) = 0.1369^{27}$, leads to $\langle 0_1||\hat{T}(E2)||2_2\rangle/\langle 2_1||\hat{T}(E2)||2_2\rangle = 0.0567^{6}$, cf. 0.0595^{18} from the adopted matrix elements in Table II. Accommodation of this datum in our evaluation has not been made because some of the multi-Coulex analyses used such a datum. Simple changes, such as "deriving" $\langle 0_1||\hat{T}(E2)||2_2\rangle$ from $\langle 2_1||\hat{T}(E2)||2_2\rangle$, do not change any of the quantitative results within the quoted uncertainties, e.g., from $\langle 2_1||\hat{T}(E2)||2_2\rangle$, $\langle 0_1||\hat{T}(E2)||2_2\rangle = 1.53^{5} \times 0.0567^{6} = 0.087^{3}$ changes Fig. 1(a) to yield, cf. Eq. (11), $(\gamma + \Gamma)' = -3.87^{14}$ deg, whence $\gamma = 19.98^{13}$ deg and $\Gamma = -23.85^{13}$ deg.

TABLE III. The ability of the model to fit the experimental $E2$ matrix elements, in e b, is shown for the $I = 0, 2$ subspace. The three model parameters used are $Q_0 = -4.155^{98}$ e b, $\gamma = 19.85^{13}$ deg, and $\Gamma = -23.92^{13}$ deg.

M.E.	Exp. (e b)	Theory (e b)	% dev.
$\langle 0_1\|\|\hat{T}(E2)\|\|2_1\rangle$	$(-)\,1.281^{9}$	$(-)\,1.307^{31}$	−2.0%
$\langle 0_1\|\|\hat{T}(E2)\|\|2_2\rangle$	$(+)\,0.091^{2}$	$(+)\,0.0928^{48}$	2.0%
$\langle 2_1\|\|\hat{T}(E2)\|\|2_2\rangle$	$(-)\,1.53^{5}$	$(-)\,1.449^{34}$	5.1%
$\langle 2_1\|\|\hat{T}(E2)\|\|2_1\rangle$	$+0.61^{6}$	$+0.595^{16}$	−3.1%
$\langle 2_2\|\|\hat{T}(E2)\|\|2_2\rangle$	-0.66^{14}	-0.595^{16}	9.6%
	Exp. (e b)^4	Theory (e b)^4	% dev.
P_4[a]	$+0.109^{11}$	$+0.105^{7}$	−4.3%

[a]The sign of the P_4 term is independent of all phase-factor conventions for the $E2$ matrix elements (unlike the P_3 term).

The model and experimental $E2$ matrix elements are compared in Table III. The model parameters yield $P_4 = +0.105^{7}$ (e b)^4; i.e., the model yields a positive value for P_4 because $\gamma < |\Gamma|$ (i.e., with respect to using the $0^\circ \leqslant \gamma \leqslant 30^\circ$ region); and, from the positive value of $\langle 2_1||\hat{T}(E2)||2_1\rangle$, the model yields a positive value for P_3.

The present work shows that the triaxial rotor model with independent inertia and electric quadrupole tensors [1] is naturally able to explain P_3 and P_4 sign anomalies. This is a new insight into collective behavior, namely that the inertia and electric quadrupole tensors result in a strong interference effect (e.g., $\gamma + \Gamma$) that is manifested in the $E2$ properties of collective nuclei. Indeed, the present study reveals the need for a better understanding of the inertia tensor in nuclei (this is a topic for a separate investigation). The result is significant also in that previously there was no simple model that could explain so-called anomalous P_3 and P_4 values. The sign of the P_3 term can play a significant role in extracting quadrupole moments of 2_1^+ states in nuclei because it can often lead to 40% uncertainties [3,4,9,13–15]. The present work suggests how to arrive at the "correct" sign for P_3. From a wider perspective, the model provides a physically insightful means for systematizing nuclear $E2$ data.

The authors thank I. Y. Lee, C. Y. Wu, and J. O. Rasmussen for useful discussions. This work was performed under the auspices of the US Department of Energy by the University of Richmond under Grants DE-FG52-06NA26206 and DE-FG02-05ER41379, and by the Georgia Institute of Technology under Grant DE-FG02-96ER40958.

[1] J. L. Wood, A. M. Oros-Peusquens, R. Zaballa, J. M. Allmond, and W. D. Kulp, Phys. Rev. C **70**, 024308 (2004).
[2] J. M. Allmond, R. Zaballa, A. M. Oros-Peusquens, W. D. Kulp, and J. L. Wood, Phys. Rev. C **78**, 014302 (2008).
[3] K. Kumar, Phys. Lett. **B29**, 25 (1969).
[4] R. J. Pryor and J. X. Saladin, Phys. Rev. C **1**, 1573 (1970).
[5] R. D. Larsen, J. A. Thomson, R. G. Kerr, R. P. Scharenberg, and W. R. Lutz, Nucl. Phys. **A195**, 119 (1972).
[6] F. T. Baker, A. Scott, T. H. Kruse, W. Hartwig, E. Ventura, and W. Savin, Phys. Rev. Lett. **37**, 193 (1976).
[7] F. T. Baker, A. Scott, T. H. Kruse, W. Hartwig, E. Ventura, and W. Savin, Nucl. Phys. **A266**, 337 (1976).
[8] F. T. Baker, A. Scott, R. M. Ronningen, T. H. Kruse, R. Suchannek, and W. Savin, Phys. Rev. C **17**, 1559 (1978).
[9] C. Fahlander, L. Hasselgren, J. E. Thun, A. Bockisch, A. M. Kleinfeld, A. Gelberg, and K. P. Lieb, Phys. Lett. **B60**, 347 (1976).
[10] L. Hasselgren, C. Fahlander, J. E. Thun, A. Bockisch, and F. J. Bergmeister, Phys. Lett. **B83**, 169 (1979).
[11] F. T. Baker, Phys. Rev. Lett. **43**, 195 (1979).
[12] F. T. Baker, Nucl. Phys. **A331**, 39 (1979).
[13] J. E. Glenn and J. X. Saladin, Phys. Rev. Lett. **20**, 1298 (1968).
[14] S. M. Burnett, A. M. Baxter, G. J. Gyapong, M. P. Fewell, and R. H. Spear, Nucl. Phys. **A494**, 102 (1989).
[15] N. J. Stone, At. Data Nucl. Data Tables **90**, 75 (2005).
[16] A. Winther and J. de Boer, in *Coulomb Excitation*, edited by K. Alder and A. Winther (Academic Press, New York, 1966).
[17] T. Tamura, Phys. Lett. **B28**, 90 (1968).
[18] V. I. Isakov and K. Kh. Lemberg, Pis'ma Zh. Eksp. Teor. Fiz. **9**, 698 (1969) [JETP Lett. **9**, 438 (1969)].
[19] C. Y. Chen, J. X. Saladin, and A. A. Hussein, Phys. Rev. C **28**, 1570 (1983).
[20] A. Bohr and B. R. Mottelson, *Nuclear Structure* (Benjamin, Reading, MA, 1975), Vol. II.
[21] A. S. Davydov and G. F. Filippov, Nucl. Phys. **8**, 237 (1958).
[22] C. S. Lim, R. H. Spear, M. P. Fewell, and G. J. Gyapong, Nucl. Phys. **A548**, 308 (1992).
[23] M. Koizumi, A. Seki, Y. Toh, M. Oshima, A. Osa, A. Kimura, Y. Hatsukawa, T. Shizuma, T. Hayakawa, M. Matsuda *et al.*, Eur. Phys. J. A **18**, 87 (2003).
[24] C. Y. Wu, D. Cline, T. Czosnyka, A. Backlin, C. Baktash, R. M. Diamond, G. D. Dracoulis, L. Hasselgren, H. Kluge, B. Kotlinski, J. R. Leigh, J. O. Newton, W. R. Phillips, S. H. Sie, J. Srebrny, and F. S. Stephens, Nucl. Phys. **A607**, 178 (1996).
[25] C. Baktash, J. X. Saladin, J. J. O'Brien, and J. G. Alessi, Phys. Rev. C **18**, 131 (1978).
[26] K. Stelzer, F. Rauch, Th. W. Elze, Ch. E. Gould, J. Idzko, G. E. Mitchell, H. P. Nottrodt, and R. Zoller, Phys. Lett. **B70**, 297 (1977).
[27] R. M. Ronningen, R. B. Piercey, A. V. Ramayya, J. H. Hamilton, S. Raman, P. H. Stelson, and W. K. Dagenhart, Phys. Rev. C **16**, 571 (1977).
[28] E. J. Bruton, J. A. Cameron, A. W. Gibb, D. B. Kenyon, and L. Keszthelyi, Nucl. Phys. **A152**, 495 (1970).
[29] G. J. Gyapong, R. H. Spear, M. T. Esat, M. P. Fewell, A. M. Baxter, and S. M. Burnett, Nucl. Phys. **A458**, 165 (1986).
[30] J. K. Sprinkle, thesis, University of Rochester, 1977, cited in Ref. [24].
[31] S. Raman, C. W. Nestor, Jr., and P. Tikkanen, At. Data Nucl. Data Tables **78**, 1 (2001).
[32] I. Berkes, R. Rougny, M. Meyer-Lévy, R. Chéry, J. Danière, G. Lhersonneau, and A. Troncy, Phys. Rev. C **6**, 1098 (1972).
[33] B. Singh, Nucl. Data Sheets **107**, 1531 (2006).